

Color Coherence Effects in Dipole-Quark Scattering in the Soft Limit

Daniel Pablos^{1,*} and Sergio Sanjurjo^{2,†}

¹*Instituto Galego de Física de Altas Enerxías IGFAE,
Universidade de Santiago de Compostela, E-15782 Galicia-Spain*

²*Departamento de Física, Universidad de Oviedo,
Avda. Federico García Lorca 18, 33007 Oviedo, Spain*

(Dated: June 14, 2024)

Color coherence effects play a crucial role in the description of jet evolution at collider experiments. It is well known that the stimulated gluon emission suffered by energetic jets traversing deconfined QCD matter is also affected by color coherence effects. Through multiple soft scatterings with the medium constituents, an antenna will lose its color correlation, causing its legs to behave as independent emitters after the so-called decoherence time. In this work we provide the first computation of the properties of the recoils produced as a result of these soft scatterings between a color coherent dipole and the medium constituents. Our findings reveal that the angular phase-space of these soft recoils is strongly restricted by the opening angle of the dipole itself due to quantum interference effects. In this long wavelength limit, one can effectively consider that interactions take place with each of the legs of the dipole separately, provided that the angular constraints dictated by the corresponding color flow topologies are respected. This is in complete analogy with the case of soft gluon emission in vacuum, where the recoil quark plays the role of the emitted gluon. As a direct phenomenological application we estimate the collisional energy loss rate of a color antenna. Importantly, these results indicate the way in which color coherence effects can be implemented in jet quenching models that account for the recoils from elastic scatterings, improving in this way our description of medium response physics in heavy-ion collisions.

I. INTRODUCTION

Color coherence phenomena are present in any gauge theory. In Quantum Chromodynamics (QCD), experimental confirmation of the detailed predictions associated to color flow topologies has contributed to validating the perturbative approach to jet physics at colliders. Salient examples include the phenomenon of drag, or string, effects [1, 2] in which the multiplicities of two- and three-jet events depend on the geometry of those jet configurations, and also the phenomenon of angular ordering (AO) in soft gluon emission [3, 4], leading to a depletion of soft particles yields around a jet due to destructive interferences, known as the humpback plateau [5]. The remarkable AO effects state that soft gluon emission off a color dipole can be effectively described as the independent emission off each of the legs of the dipole provided that one observes certain restrictions in the angular phase-space of the emission. This picture provides the basis of the probabilistic approach to the simulation of jet evolution used in modern event generators [6].

The evolution of jets traversing deconfined QCD matter, such as the quark-gluon plasma (QGP) created in heavy-ion collisions, has also been shown to be affected by coherence effects. Stimulated gluon emission via repeated scatterings with the medium constituents [7–15] leads to a degradation of the jet energy and a modification of its substructure, a set of phenomena commonly referred to as jet quenching [16–19]. The study of the

bremsstrahlung pattern off a color dipole [20–25] revealed that each leg will behave as an independent emitter only after the decoherence time τ_d , when independent color rotations have led to a loss of the color coherence of the pair. While much is known about the description of medium-induced radiation off a color dipole and its phenomenological consequences [26–41], this is not the case for the description of the medium constituents after the multiple soft scatterings take place. This is largely due to the fact that the importance of these recoils has only been acknowledged relatively recently (see [42] and references therein). Interesting on their own right as a means to learn about the inner workings of the QGP at various length scales [43–46], they appear to be crucial in the description of most jet observables [47–52]. They contribute as correlated background, influencing the way we interpret jet quenching phenomena in experiments and thus affecting our ability to understand the various physical mechanisms at play.

This Letter addresses, for the first time, the coherence effects on the properties of the medium recoils involved in scattering with a color-coherent energetic dipole. Using standard perturbative techniques, we show in Section II that the angular distribution of those recoils is strongly influenced by interference phenomena, closely resembling the patterns found for soft gluon emission. These results allow us to provide an estimate for the collisional energy loss rate of a color dipole in Section III. Finally, in Section IV we look ahead and comment on the implications of these results in the modelling of elastic collisions in jet quenching event generators.

* daniel.pablos@usc.es

† sergiosanjurjom@gmail.com

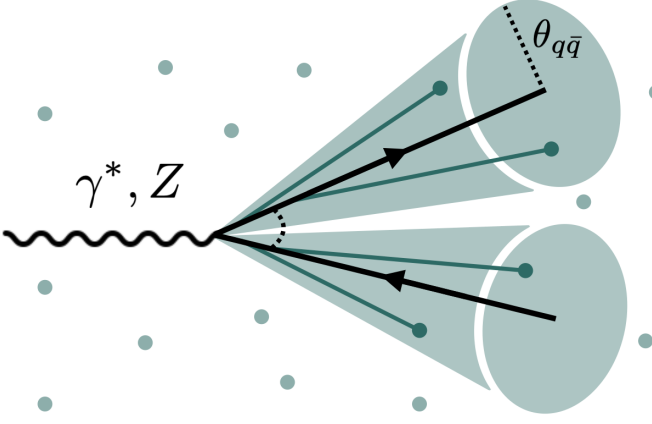


FIG. 1. Sketch representing a color singlet dipole (solid black lines) produced by the decay of a colorless boson (wiggly black line) that interacts with some medium constituents (green dots). Quantum interference effects restrict the recoil angles (green lines ending with dots) to lie within cones of the angular size of the dipole, $\theta_{q\bar{q}}$ (dotted black lines), centered at each of the dipole legs.

II. COLOR DIPOLE SCATTERING WITH A QUARK IN THE SOFT LIMIT

A. $\gamma^* \rightarrow q\bar{q}$ Antenna

We will look first at the scattering process between a soft quark and a virtual photon that decays into a $q\bar{q}$ pair. The quark is soft both regarding its rest mass m and the energy E acquired in the scattering (assuming $m \ll E$) with the energetic dipole with total energy w . We consider those diagrams that are leading in $\beta = E/w$. The two leading diagrams are those with a scattering with either the quark or the anti-quark by the exchange of a virtual gluon in the t -channel. All other diagrams (s -channel as well as u -channel contributions) are suppressed in the soft limit we are interested in. Using Feynman rules in momentum space, the t -channel diagrams read

$$i\mathcal{M}_1^\gamma = \frac{-ig_s^2 eQ}{q^2} a_{ij} a_{kl} \left[\bar{u}(s) \gamma^\mu \not{f} \Gamma v(\bar{s}) \right] [\bar{u}(p') \gamma_\mu u(p)] \quad (1)$$

$$i\mathcal{M}_2^\gamma = \frac{-ig_s^2 eQ}{q^2} a_{ij} a_{kl} \left[\bar{u}(s) \Gamma \frac{-\not{f}}{\bar{r}^2} \gamma^\mu v(\bar{s}) \right] [\bar{u}(p') \gamma_\mu u(p)] , \quad (2)$$

where p is the momentum of the incoming quark, p' is the momentum of the outgoing quark, $q = p' - p$ is the exchanged momentum with the antenna, s is the momentum of the quark of the antenna, \bar{s} is the momentum of the anti-quark of the antenna, $r = q + s$ is the momentum in the virtual quark propagator and $\bar{r} = q + \bar{s}$ is the momentum in the virtual anti-quark propagator. The term Γ represents the interaction vertex associated

to the origination of the dipole. eQ is the electric charge carried by the quarks of the antenna and g_s is the strong coupling constant. The latin indices ij and kl in the fundamental representation indicate the color flow in the soft quark and antenna, respectively. We are working in the Feynman gauge.

Regarding the algebra of the legs of the dipole, we assume that the exchanged momentum is small and use the equations of motion for a massless quark, so $\not{f}u(s) \approx \not{f}u(s) = 0$, and analogously for the anti-quark. The sum of the two matrix elements is (using $\{\gamma^\mu, \gamma^\nu\} = 2g^{\mu\nu}$)

$$i\mathcal{M}^\gamma = i\mathcal{M}_1^\gamma + i\mathcal{M}_2^\gamma = \frac{-2g_s^2}{q^2} a_{ij} a_{kl} B^\mu \left(\frac{s_\mu}{r^2} - \frac{\bar{s}_\mu}{\bar{r}^2} \right) \Gamma_{q\bar{q}}^\gamma , \quad (3)$$

where we have defined $B^\mu \equiv \bar{u}(p') \gamma^\mu u(p)$. Here, $\Gamma_{q\bar{q}}^\gamma \equiv ieQ \bar{u}(s) \Gamma v(\bar{s})$, and its explicit form is not relevant for our present discussion as it is factorized from the rest of the expression in the soft limit. Averaging over initial color states (N possible colors for the incoming quark) and summing over final color states, the color factor gives

$$\frac{1}{N} \sum (t_{ij}^a t_{kl}^a)^* (t_{ij}^b t_{kl}^b) = \frac{C_F}{2} . \quad (4)$$

Averaging over initial and summing over final spin polarizations leads us to the unpolarized squared matrix element

$$|\mathcal{M}_{q\bar{q}}^\gamma|^2 = \frac{4g_s^4}{q^4} \Omega_{q\bar{q}}^\gamma \frac{C_F}{2} A^{\mu\nu} B_{\mu\nu} \equiv \Omega_{q\bar{q}}^\gamma |\mathcal{S}_{q\bar{q}}^\gamma|^2 , \quad (5)$$

with the antenna current $A^{\mu\nu}$

$$A^{\mu\nu}(p, p', s, \bar{s}) = \frac{s^\mu s^\nu}{r^4} - 2 \frac{\bar{s}^\mu s^\nu}{\bar{r}^2 r^2} + \frac{\bar{s}^\mu \bar{s}^\nu}{\bar{r}^4} , \quad (6)$$

and the recoil quark current $B^{\mu\nu}$

$$\begin{aligned} B^{\mu\nu}(p, p') &= \frac{1}{2} \text{Tr}(\not{p} \gamma^\mu \not{p}' \gamma^\nu) = \\ &= 2(p^\mu p'^\nu + p'^\mu p^\nu - g^{\mu\nu} p \cdot p') . \end{aligned} \quad (7)$$

The antenna production term $\Omega_{q\bar{q}}^\gamma$ depends solely on $\Gamma_{q\bar{q}}^\gamma$. We now separate the antenna current $A^{\mu\nu}$ into two terms, $A^{\mu\nu} = A_s^{\mu\nu} + A_{\bar{s}}^{\mu\nu}$, with

$$A_s^{\mu\nu} \equiv \frac{s^\mu s^\nu}{r^4} - \frac{\bar{s}^\mu s^\nu}{r^2 \bar{r}^2} \quad (8)$$

and analogously for $A_{\bar{s}}^{\mu\nu}$ by interchanging s and \bar{s} . We are at a reference frame where the target quark is at rest, with rest mass m . We take m to be the smallest scale in the problem. The energy of the recoiling quark is $\sqrt{E^2 + m^2}$. By taking the $m \rightarrow 0$ limit, we can approximate the propagators as

$$\begin{aligned} q^2 &= (p' - p)^2 \approx -2Em + \mathcal{O}(m^2) \\ r^2 &= q^2 + 2q \cdot s \approx 2p' \cdot s + \mathcal{O}(m) \\ \bar{r}^2 &= q^2 + 2q \cdot \bar{s} \approx 2p' \cdot \bar{s} + \mathcal{O}(m) . \end{aligned} \quad (9)$$

Contraction of one of the antenna currents with the current $B^{\mu\nu}(p, p')$ yields

$$W_s \equiv A_s^{\mu\nu} B_{\mu\nu} = \frac{1}{2} \left(\frac{p \cdot s}{p' \cdot s} - \frac{p \cdot \bar{s}}{p' \cdot \bar{s}} + \frac{(p \cdot p')(s \cdot \bar{s})}{(p' \cdot s)(p' \cdot \bar{s})} \right). \quad (10)$$

We readily recognize the well-known pattern found in the context of soft gluon emission [3, 4], where the recoil quark p' plays the role of the emitted gluon

$$W_s = \frac{m}{2E} \left(\frac{1}{1 - \cos \theta_{p's}} - \frac{1}{1 - \cos \theta_{p'\bar{s}}} + \frac{1 - \cos \theta_{s\bar{s}}}{(1 - \cos \theta_{p's})(1 - \cos \theta_{p'\bar{s}})} \right). \quad (11)$$

W_s ($W_{\bar{s}}$) possesses an angular divergence only when the angle between the recoil quark and the quark (anti-quark) leg goes to zero, i.e. $\theta_{p's}(\theta_{p'\bar{s}}) \rightarrow 0$, and can be reinterpreted as describing the interaction with just the quark (anti-quark) leg. By aligning the reference frame with respect to the quark s , and integrating the recoil quark p' over the azimuthal angle ϕ one gets

$$\int \frac{d\phi}{2\pi} W_s = \frac{m}{E} \frac{1}{1 - \cos \theta_{p's}} \Theta(\theta_{s\bar{s}} - \theta_{p's}), \quad (12)$$

enforcing the recoil quark angle to lie within a cone of the size of the angle of the dipole centered around the quark leg. These results are illustrated in Fig. 1. Perhaps an interesting fact is that, in contrast to the soft emission calculation, the squared of the individual matrix elements is non-vanishing and naturally provides the necessary terms to construct W_s and $W_{\bar{s}}$ [53].

Just as in the soft emission scenario, these physics can be heuristically discussed in terms of the so-called Chudakov effect [54] in cosmic ray physics. By virtue of the Heisenberg uncertainty principle, the lifetime of the virtual quark carrying momentum $r = s + q$ is $\Delta t \sim 1/\Delta E$, with $\Delta E = |s| + |q| - |r| \sim E\theta^2 = \theta/\lambda_T$, with λ_T the wavelength of the recoil quark transverse to the dipole quark. In order to resolve the dipole internal structure, λ_T needs to be smaller than the dipole opening d after the virtual quark lifetime, so $d = \theta_{q\bar{q}}\Delta t = \theta_{q\bar{q}}\lambda_T/\theta > \lambda_T$, and then $\theta < \theta_{q\bar{q}}$.

B. $g \rightarrow q\bar{q}$, $q \rightarrow qg$ and $g \rightarrow gg$ Antennas

We now move to the computation of the matrix elements between a dipole and a soft quark for the rest of possible color configurations.

$g \rightarrow q\bar{q}$. We start by replacing the incoming virtual photon with a virtual gluon. The two leading diagrams from the previous calculation become

$$i\mathcal{M}_1^g + i\mathcal{M}_2^g = \frac{-2g_s^2}{q^2} B^\mu a_{ij} \left\{ (ab)_{kl} \frac{s^\mu}{r^2} - (ba)_{kl} \frac{\bar{s}^\mu}{\bar{r}^2} \right\} \Gamma_{q\bar{q}}^g, \quad (13)$$

where now $\Gamma_{q\bar{q}}^g \equiv ig_s \bar{u}(s)\Gamma v(\bar{s})$. The new diagram we need to consider, namely the interaction with the incoming gluon, is notably simplified in the limit in which one of the legs carries soft momenta ($q \ll s + \bar{s}$), enhancing the term that preserves incoming gluon polarization. Within this approximation, it reads

$$i\mathcal{M}_3^g = \frac{2g_s^2}{q^2} a_{ij} [a, b]_{kl} B^\mu \left(\frac{s_\mu + \bar{s}_\mu}{k^2} \right) \Gamma_{q\bar{q}}^g. \quad (14)$$

However, it is not enhanced in the soft limit, since $k^2 \sim \mathcal{O}(\beta^0)$, and is thus a subleading contribution that we drop. Therefore, $i\mathcal{M}_{q\bar{q}}^g \approx i\mathcal{M}_1^g + i\mathcal{M}_2^g$ to leading order in β .

Averaging over initial color states (N possible colors for the incoming quark and $N^2 - 1$ for the incoming gluon) and summing over final color states, we recognize two types of color flows. The direct color flow terms yield

$$\frac{1}{N(N^2 - 1)} \sum (t_{ij}^a (t^a t^b)_{kl})^* (t_{ij}^c (t^c t^b)_{kl}) = \frac{C_F}{4N}. \quad (15)$$

The cross color flow terms yield

$$\frac{1}{N(N^2 - 1)} \sum (t_{ij}^a (t^a t^b)_{kl})^* (t_{ij}^c (t^b t^c)_{kl}) = \frac{C_F}{4N} - \frac{1}{8}. \quad (16)$$

The unpolarized squared matrix element is then

$$|\mathcal{M}_{q\bar{q}}^g|^2 = \frac{4g_s^4}{q^4} \Omega_{q\bar{q}}^g \frac{1}{4N} B_{\mu\nu} \left[C_F A^{\mu\nu} + C_A \frac{s^\mu \bar{s}^\nu}{r^2 \bar{r}^2} \right], \quad (17)$$

where $\Omega_{q\bar{q}}^g$ is again associated to dipole production. The term proportional to C_F presents, as before, a recoil quark with an angle contained *within* the cone of the $q\bar{q}$ antenna centered around each of the legs. The new term $s^\mu \bar{s}^\nu / r^2 \bar{r}^2 \equiv J^{\mu\nu}$, proportional to C_A , enforces a recoil angle θ

$$\int \frac{d\phi}{2\pi} J^{\mu\nu} B_{\mu\nu} = \frac{m}{E} \frac{1}{1 - \cos \theta} \Theta(\theta - \theta_{s\bar{s}}), \quad (18)$$

exclusively *outside* of the cone of the dipole centered around each of the legs, as if the scattering took place with the total charge of the dipole.

$q \rightarrow qg$. For the $q \rightarrow qg$ antenna, the sum of the leading matrix elements yields (with \bar{s} the momentum of the outgoing gluon)

$$i\mathcal{M}_{qg}^q = \frac{-2g_s^2}{q^2} B^\mu a_{ij} \left\{ (ab)_{kl} \frac{s^\mu}{r^2} - [a, b]_{kl} \frac{\bar{s}^\mu}{\bar{r}^2} \right\} \Gamma_{qg}^q, \quad (19)$$

where we have defined $\Gamma_{qg}^q \equiv ig_s \bar{u}(s)\epsilon_\alpha^*(\bar{s})\Gamma^\alpha$. Again, the diagram that describes the interaction with the incoming virtual quark is subleading in β and is neglected.

The unpolarized squared matrix element is

$$|\mathcal{M}_{qg}^q|^2 = \frac{4g_s^4}{q^4} \Omega_{qg}^q B_{\mu\nu} \frac{C_F}{2N} \left[C_F \frac{s^\mu s^\nu}{r^4} + C_A A_{\bar{s}}^{\mu\nu} \right],$$

with Ω_{gg}^g associated to the production of the dipole. We observe that there is no angular restriction for the C_F term (as if the scattering took place with the quark leg of the dipole, which is also the total charge of the dipole), while in the C_A term coherence restricts the angular distribution of the recoil to be within the cone of the dipole centered around the gluon (as if the scattering took place with the gluon leg of the dipole).

$g \rightarrow gg$. In the soft limit, the sum of the two leading matrix elements is simply (with s^μ and \bar{s}^μ the momenta of the outgoing gluons)

$$i\mathcal{M}_{gg}^g = \frac{2ig_s^2}{q^2} \Gamma_{gg}^g B_\mu a_{ij} \left\{ \frac{s^\mu}{r^2} f^{abc} f^{bed} + \frac{\bar{s}^\mu}{\bar{r}^2} f^{abe} f^{bdc} \right\}, \quad (20)$$

with $\Gamma_{gg}^g \equiv g_s \epsilon_\alpha^*(s) \epsilon_\beta^*(\bar{s}) \Gamma^{\alpha\beta}$. The direct color flow terms yield

$$\frac{1}{N(N^2-1)} \sum (t_{ij}^a f^{abc} f^{bed})^* (t_{ij}^g f^{ghc} f^{hed}) = \frac{C_A}{2}, \quad (21)$$

and the cross ones

$$\frac{1}{N(N^2-1)} \sum (t_{ij}^a f^{abc} f^{bed})^* (t_{ij}^g f^{ghe} f^{hdc}) = -\frac{C_A}{4}. \quad (22)$$

The unpolarized squared matrix element is then

$$\begin{aligned} |\mathcal{M}_{gg}^g|^2 &= \frac{4g_s^4}{q^4} \Omega_{gg}^g B_{\mu\nu} \frac{C_A}{2} \left[\frac{s^\mu s^\nu}{r^4} + \frac{\bar{s}^\mu \bar{s}^\nu}{\bar{r}^4} - \frac{s^\mu \bar{s}^\nu}{r^2 \bar{r}^2} \right] = \\ &= \frac{4g_s^4}{q^4} \Omega_{gg}^g B_{\mu\nu} \frac{C_A}{2} [A^{\mu\nu} + J^{\mu\nu}], \end{aligned} \quad (23)$$

where $A^{\mu\nu}$ enforces scattering angles within a cone centered around each of the gluon legs and $J^{\mu\nu}$ corresponds to out-of-cone recoil angles, as expected from the total charge of the antenna.

We can compactly express all previous results in the following way [23]

$$\begin{aligned} |\mathcal{M}_i|^2 &= \frac{4g_s^4}{q^4} \Omega_i C_i B_{\mu\nu} \\ &\times (u^\mu u^\nu Q_u^2 + v^\mu v^\nu Q_v^2 + 2u^\mu v^\nu Q_u \cdot Q_v), \end{aligned} \quad (24)$$

where u and v represent the two legs of the antenna $u^\mu \equiv s^\mu/r^2$, $v^\mu \equiv \bar{s}^\mu/\bar{r}^2$. The corresponding charge vectors satisfy $Q_u + Q_v = Q_t$, where Q_t is the charge of the incoming virtual object, $Q_q^2 = Q_{\bar{q}}^2 = C_F$ and $Q_g^2 = C_A$. By solving for $Q_u \cdot Q_v$ using the equation $(Q_u + Q_v)^2 = Q_t^2$ one recovers all the possible color configurations. The index i labels the four different cases, for which we have different dipole production terms Ω_i and different global color factors $C_i = \{1/2, 1/4N, C_F/2N, 1/2\}$ for processes $i = \{qq\bar{q}, gq\bar{q}, qqg, ggg\}$, respectively.

III. COLLISIONAL ENERGY LOSS OF A COLOR SINGLET DIPOLE

A quantity of interest that we can now compute is the collisional energy loss rate of a color dipole. As a simple test case, we do so for the dipole produced by the decay of a Z boson, which closely resembles that of the virtual photon since it corresponds to a color singlet antenna. The matrix element reads

$$i\mathcal{M}^Z = \frac{-2g_s^2}{q^2} a_{ij} a_{kl} B^\mu \left(\frac{s_\mu}{r^2} - \frac{\bar{s}_\mu}{\bar{r}^2} \right) \Gamma_{q\bar{q}}^Z, \quad (25)$$

where $\Gamma_{q\bar{q}}^Z = ig_Z \bar{u}(s) \not{\epsilon}(k) (g_V - g_A \gamma^5) v(\bar{s})$, with the electroweak couplings

$$g_Z = \frac{e}{\sin\theta_W \cos\theta_W}, \quad g_V = \frac{I_3}{2} - Q \sin^2\theta_W, \quad g_A = \frac{I_3}{2}, \quad (26)$$

where I_3 is the isospin of the quarks forming the antenna and θ_W is the Weinberg angle of the electroweak interaction. The unpolarized squared matrix element is

$$|\mathcal{M}_{q\bar{q}}^Z|^2 = \Omega_{q\bar{q}}^Z |\mathcal{S}_{q\bar{q}}^Z|^2, \quad (27)$$

with $|\mathcal{S}_{q\bar{q}}^Z|^2 = |\mathcal{S}_{q\bar{q}}^\gamma|^2$ and

$$\begin{aligned} \Omega_{q\bar{q}}^Z &= g_Z^2 \text{Tr}(\not{s} \gamma^\mu (g_V - g_A \gamma^5) \not{k} (g_V - g_A \gamma^5) \gamma^\nu) \\ &\times \frac{1}{3} \sum_\lambda \epsilon_\mu^\lambda(k) \epsilon_\nu^{\lambda*}(k) = \\ &= \frac{1}{3} g_Z^2 (g_V^2 - g_A^2) \text{Tr}(\not{s} \gamma^\mu \not{k} \gamma^\nu) \left(-g_{\mu\nu} + \frac{k_\mu k_\nu}{k^2} \right) \approx \\ &\approx \frac{8}{3} g_Z^2 (g_V^2 - g_A^2) s \cdot \bar{s}. \end{aligned} \quad (28)$$

The differential cross-section of the whole process factorizes into the decay rate of the Z boson into a $q\bar{q}$ antenna, $d\Gamma_Z$, and the scattering process between the color dipole and the quark, as

$$d\sigma = d\Gamma_Z \frac{2w}{4F} |\mathcal{S}_{q\bar{q}}^Z|^2 \frac{d^3 p'}{(2\pi)^3 2E}, \quad (29)$$

where $F = m\sqrt{w^2 - M^2}$ with $M \approx \sqrt{2s \cdot \bar{s}}$ the mass of the Z . The Z decay rate is

$$d\Gamma_Z = \frac{\Omega_{q\bar{q}}^Z}{2w} \frac{d^3 s}{(2\pi)^3 2w_s} \frac{d^3 \bar{s}}{(2\pi)^3 2w_{\bar{s}}} (2\pi)^4 \delta^{(4)}(s + \bar{s} - k). \quad (30)$$

Taking the term that is interpreted as the interaction with the quark leg of the antenna, we write

$$d\sigma_q = d\Gamma_Z \frac{w}{2F} \frac{C_F}{2} \frac{4g_s^4}{q^4} d\theta \frac{\sin\theta}{16\pi^3} W_s d\phi E dE, \quad (31)$$

where θ is the angle between the recoil quark and the quark leg. Performing the integration in ϕ yields

$$d\sigma_q = d\Gamma_Z \frac{w}{F} \frac{C_F}{2} \alpha_s^2 \frac{dE}{mE^2} d\theta \cot(\theta/2) \Theta(\theta_{q\bar{q}} - \theta), \quad (32)$$

where we have used the result from Eq. (12) and $q^4 \approx 4m^2 E^2$. Note that the soft divergence associated to the propagator q^4 , E^{-2} , actually corresponds to the typical angular divergence of a Rutherford scattering, since no exchanged momentum ($E \rightarrow 0$) would translate into zero deflection of the corresponding leg of the antenna. Comparing the final soft divergence of the cross-section, dE/E^2 , to the soft divergence of gluon emission, dE/E , we understand the difference as arising from an extra factor of $1/E$ from Eq. (12), which is absent in the soft gluon emission computation.

The scattering rate is equal to the cross-section times the density of scatterers, $d\Gamma_q = nd\sigma_q$. The total (accounting for the two legs of the dipole) average energy loss per unit length dE_T/dx is thus

$$\begin{aligned} \frac{dE_T}{dx} &= 2\langle E d\Gamma_q \rangle = \\ &= 2d\Gamma_Z \frac{w}{F} \frac{C_F}{2} \frac{n}{m} \mathcal{A}(\theta_0, \theta_{q\bar{q}}) \mathcal{E}(E_M, E_m), \end{aligned} \quad (33)$$

where the integral over the recoil energy E over a minimum energy (E_m , which relates to the angular cut-off of the t -channel propagator) and maximum energy ($E_M \ll w$) is

$$\begin{aligned} \mathcal{E}(E_M, E_m) &\equiv \int_{E_m}^{E_M} \frac{dE}{E} \alpha_s^2(|q|) = \\ &= \frac{16\pi^2}{\beta_0^2} \frac{\log \frac{E_M}{E_m}}{\log \frac{2E_m^2}{Q_0^2} \log \frac{2E_M E_m}{Q_0^2}}, \end{aligned} \quad (34)$$

and we have used the expression $\alpha_s(\mu) = 2\pi/\beta_0 \log(\mu/Q_0)$ for the running coupling constant. In the small angle limit, the angular integral is

$$\mathcal{A}(\theta_0, \theta_{q\bar{q}}) \approx 2 \log \frac{\theta_{q\bar{q}}}{\theta_0}. \quad (35)$$

This is the divergence associated to the virtual propagators in the dipole, occurring when the recoil is collinear with the corresponding leg, and is absent when one considers an elastic scattering between an on-shell parton, coming from infinity, and the soft quark. Retaining the masses of the quarks of the antenna in the propagator naturally regulates this divergence. In the case of soft gluon emissions, this mass singularity is regulated by the inclusion of the virtual contributions. A more careful discussion of the treatment of these divergences for the case of dipole-quark scattering, possibly including the so-called contact terms that result into a zero-point subtraction prescription, is left for future work.

The restriction of the angular phase-space of the recoiling quark reduces the amount of collisional energy loss for narrower antennas as compared to wider ones. This is so until the dipole decoheres at time τ_d , after which collisional energy loss of the system increases, just as radiative energy loss does [26]. As per the effects of collisional energy loss, one expects that those Z bosons with decay

products that are widely separated will lead, on average, to smaller values of the Z reconstructed mass (ignoring any possible effects from broadening) than those with narrower angles. These features can be analyzed by expressing the Z decay rate, Eq. (30), in terms of the angle and energies of the decay products, i.e. $d\Gamma_Z/d\theta_{q\bar{q}}dw_s dw_{\bar{s}}$. A detailed phenomenological study that can complement the proposal to measure the shift of the W boson mass due to radiative energy loss [55] is left to future work.

IV. SUMMARY AND OUTLOOK

In this Letter we have computed the cross-section for the scattering process between a color dipole and a quark at rest. We have found that, in the soft limit, i.e. when $E \ll w$, with E the energy of the recoiling quark and w the total energy of the dipole, the angular phase-space of the recoiling quark depends on the opening angle of the dipole itself due to quantum interference effects. In this long wavelength limit the recoil quark behaves classically and interactions can be effectively arranged as if they took place with the different color charges of the dipole separately, provided one respects the angular constraints. This is in complete analogy to the physics found in the context of soft gluon emission off a color dipole [3, 4], where the recoiling quark plays the role of the soft gluon.

Within a dense medium, such as the QGP created in heavy-ion collisions, an energetic parton frequently experiences such soft scatterings, leading to radiative energy loss. It has been common practice to treat these interactions in the limit in which the medium scattering centres have infinite mass (with some recent notable exceptions where the ensembles of scattering centres can be inhomogeneous [56–60] and non-static [60–62]), neglecting back-reaction and thus justifying the modelling of the medium as a stochastic, classical background field. This simplification facilitates the resummation of an infinite number of these scatterings, allowing for a convenient reformulation of the problem in terms of Wilson lines. Under this framework, it has been shown that these multiple soft scatterings can lead to color decoherence between the two legs of a dipole after a timescale τ_d [21, 22, 24, 63]. In the present work we have focused on the properties of the recoiling partons that participate in soft scatterings, which obviously means that we have had to consider back-reaction on the medium constituents. These differences in the medium modelling assumptions between all previous work, addressing dipole color decoherence, and the present work, addressing imprints of color coherence in the recoil properties, motivates further work to establish a comprehensive framework to simultaneously address both phenomena.

The clear message from the results here presented is that, as long as a dipole is in a color coherent state, recoils produced in soft scatterings are restricted to lie at the angular regions allowed by color coherence effects. This picture suggests a way forward towards implement-

ing color coherence effects in the modelling of elastic collisions in jet quenching models. Crucially, high-energy partons produced during jet evolution *cannot* in general be considered as on-shell states coming from infinity, and their correct description is in terms of a collection of color correlated dipoles. A number of such models already incorporate the dynamics of recoils [64–68], but do not account for color coherence effects whatsoever as they work using on-shell states. In order to include such effects, one could in principle consider elastic scatterings off each of the legs of a given dipole independently, by sampling a collisional rate $d\Gamma_g$, ensuring that they respect the angular constraints illustrated in, e.g., Eq. (12), Eq. (18), or no constraint at all, depending on the specific color flow topology – as long as they are in a color coherent state (namely if time $\tau < \tau_d$). For the case of a color singlet antenna, this implies that while the dipole is being decohered via multiple soft scatterings, a number of soft recoils appear strictly around the cone of the dipole, drawing the shape of the antenna, while no stimulated gluon emission can take place. When the dipole decoheres, recoils no longer have an angular restriction, and stimulated emission off the individual quark legs can occur. A dedicated phenomenological study using jet quenching Monte Carlos will be done in future work.

We anticipate that the results from this Letter will

be important in improving the theoretical description of high-energy jets traversing deconfined QCD media, such as the QGP created in heavy-ion collisions. A better understanding of the recoils involved in elastic scatterings with the color-coherent multi-partonic structures generated by jet evolution is crucial for characterizing medium response physics and, by extension, for understanding the nature of the QGP itself.

ACKNOWLEDGMENTS

We are thankful to Néstor Armesto, João Barata, Jorge Casalderrey-Solana, Fabio Domínguez, Xabier Feal, Xoán Mayo López, Mateusz Ploskon, Krishna Rajagopal, Diego Rodríguez-López, Andrey Sadofyev, Carlos Salgado and Konrad Tywoniuk for helpful discussions. DP is funded by the European Union’s Horizon 2020 research and innovation program under the Marie Skłodowska-Curie grant agreement No 101155036 (AntScat), by the European Research Council project ERC-2018-ADG-835105 YoctoLHC, by Spanish Research State Agency under project PID2020-119632GB-I00, by Xunta de Galicia (CIGUS Network of Research Centres) and the European Union, and by Unidad de Excelencia María de Maetzu under project CEX2023-001318-M.

-
- [1] Y. L. Dokshitzer, V. A. Khoze, S. I. Troian, and A. H. Mueller, *Rev. Mod. Phys.* **60**, 373 (1988).
- [2] Y. L. Dokshitzer, V. A. Khoze, A. H. Mueller, and S. Troian, *Basics of perturbative QCD* (Editions Frontières, Gif-sur-Yvette, 1991).
- [3] A. H. Mueller, *Phys. Lett. B* **104**, 161 (1981).
- [4] B. I. Ermolaev and V. S. Fadin, *JETP Lett.* **33**, 269 (1981).
- [5] Y. I. Azimov, Y. L. Dokshitzer, V. A. Khoze, and S. I. Troian, *Z. Phys. C* **31**, 213 (1986).
- [6] G. Marchesini and B. R. Webber, *Nucl. Phys. B* **238**, 1 (1984).
- [7] R. Baier, Y. L. Dokshitzer, A. H. Mueller, S. Peigne, and D. Schiff, *Nucl. Phys. B* **483**, 291 (1997), [arXiv:hep-ph/9607355](#).
- [8] R. Baier, Y. L. Dokshitzer, A. H. Mueller, S. Peigne, and D. Schiff, *Nucl. Phys. B* **484**, 265 (1997), [arXiv:hep-ph/9608322](#).
- [9] B. G. Zakharov, *JETP Lett.* **63**, 952 (1996), [arXiv:hep-ph/9607440](#).
- [10] B. G. Zakharov, *JETP Lett.* **65**, 615 (1997), [arXiv:hep-ph/9704255](#).
- [11] M. Gyulassy, P. Levai, and I. Vitev, *Phys. Rev. Lett.* **85**, 5535 (2000), [arXiv:nucl-th/0005032](#).
- [12] M. Gyulassy, P. Levai, and I. Vitev, *Nucl. Phys. B* **594**, 371 (2001), [arXiv:nucl-th/0006010](#).
- [13] U. A. Wiedemann, *Nucl. Phys. B* **588**, 303 (2000), [arXiv:hep-ph/0005129](#).
- [14] X.-N. Wang and X.-f. Guo, *Nucl. Phys. A* **696**, 788 (2001), [arXiv:hep-ph/0102230](#).
- [15] M. Djordjevic and M. Gyulassy, *Nucl. Phys. A* **733**, 265 (2004), [arXiv:nucl-th/0310076](#).
- [16] D. d’Enterria, *Landolt-Bornstein* **23**, 471 (2010), [arXiv:0902.2011 \[nucl-ex\]](#).
- [17] U. A. Wiedemann, *Phys. Lett. B* **521** (2010), [arXiv:0908.2306 \[hep-ph\]](#).
- [18] A. Majumder and M. Van Leeuwen, *Prog. Part. Nucl. Phys.* **66**, 41 (2011), [arXiv:1002.2206 \[hep-ph\]](#).
- [19] Y. Mehtar-Tani, J. G. Milhano, and K. Tywoniuk, *Int. J. Mod. Phys. A* **28**, 1340013 (2013), [arXiv:1302.2579 \[hep-ph\]](#).
- [20] Y. Mehtar-Tani, C. A. Salgado, and K. Tywoniuk, *Phys. Rev. Lett.* **106**, 122002 (2011), [arXiv:1009.2965 \[hep-ph\]](#).
- [21] J. Casalderrey-Solana and E. Iancu, *JHEP* **08**, 015 (2011), [arXiv:1105.1760 \[hep-ph\]](#).
- [22] Y. Mehtar-Tani, C. A. Salgado, and K. Tywoniuk, *Phys. Lett. B* **707**, 156 (2012), [arXiv:1102.4317 \[hep-ph\]](#).
- [23] Y. Mehtar-Tani, C. A. Salgado, and K. Tywoniuk, *JHEP* **04**, 064 (2012), [arXiv:1112.5031 \[hep-ph\]](#).
- [24] Y. Mehtar-Tani, C. A. Salgado, and K. Tywoniuk, *JHEP* **10**, 197 (2012), [arXiv:1205.5739 \[hep-ph\]](#).
- [25] J. Casalderrey-Solana, D. Pablos, and K. Tywoniuk, *JHEP* **11**, 174 (2016), [arXiv:1512.07561 \[hep-ph\]](#).
- [26] J. Casalderrey-Solana, Y. Mehtar-Tani, C. A. Salgado, and K. Tywoniuk, *Phys. Lett. B* **725**, 357 (2013), [arXiv:1210.7765 \[hep-ph\]](#).
- [27] Y. Mehtar-Tani and K. Tywoniuk, *JHEP* **04**, 125 (2017), [arXiv:1610.08930 \[hep-ph\]](#).
- [28] Y. Mehtar-Tani and K. Tywoniuk, *Phys. Rev. D* **98**, 051501 (2018), [arXiv:1707.07361 \[hep-ph\]](#).
- [29] Z. Hulcher, D. Pablos, and K. Rajagopal, *JHEP* **03**, 010 (2018), [arXiv:1707.05245 \[hep-ph\]](#).

- [30] P. Caucal, E. Iancu, A. H. Mueller, and G. Soyez, *Phys. Rev. Lett.* **120**, 232001 (2018), [arXiv:1801.09703 \[hep-ph\]](#).
- [31] P. Caucal, E. Iancu, and G. Soyez, *JHEP* **10**, 273 (2019), [arXiv:1907.04866 \[hep-ph\]](#).
- [32] J. Casalderrey-Solana, G. Milhano, D. Pablos, and K. Rajagopal, *JHEP* **01**, 044 (2020), [arXiv:1907.11248 \[hep-ph\]](#).
- [33] P. Caucal, E. Iancu, A. H. Mueller, and G. Soyez, *JHEP* **10**, 204 (2020), [arXiv:2005.05852 \[hep-ph\]](#).
- [34] Y. Mehtar-Tani, D. Pablos, and K. Tywoniuk, *Phys. Rev. Lett.* **127**, 252301 (2021), [arXiv:2101.01742 \[hep-ph\]](#).
- [35] P. Caucal, A. Soto-Ontoso, and A. Takacs, *Phys. Rev. D* **105**, 114046 (2022), [arXiv:2111.14768 \[hep-ph\]](#).
- [36] D. Pablos and A. Soto-Ontoso, *Phys. Rev. D* **107**, 094003 (2023), [arXiv:2210.07901 \[hep-ph\]](#).
- [37] R. Belmont *et al.*, *Nucl. Phys. A* **1043**, 122821 (2024), [arXiv:2305.15491 \[nucl-ex\]](#).
- [38] C. Andres, F. Dominguez, R. Kunnawalkam Elayavalli, J. Holguin, C. Marquet, and I. Moulton, *Phys. Rev. Lett.* **130**, 262301 (2023), [arXiv:2209.11236 \[hep-ph\]](#).
- [39] C. Andres, F. Dominguez, J. Holguin, C. Marquet, and I. Moulton, *JHEP* **09**, 088 (2023), [arXiv:2303.03413 \[hep-ph\]](#).
- [40] L. Cunqueiro, D. Pablos, A. Soto-Ontoso, M. Spusta, A. Takacs, and M. Verweij, (2023), [arXiv:2311.07643 \[hep-ph\]](#).
- [41] Y. Mehtar-Tani, D. Pablos, and K. Tywoniuk, (2024), [arXiv:2402.07869 \[hep-ph\]](#).
- [42] S. Cao and X.-N. Wang, *Rept. Prog. Phys.* **84**, 024301 (2021), [arXiv:2002.04028 \[hep-ph\]](#).
- [43] F. D'Eramo, M. Lekaveckas, H. Liu, and K. Rajagopal, *JHEP* **05**, 031 (2013), [arXiv:1211.1922 \[hep-ph\]](#).
- [44] F. D'Eramo, K. Rajagopal, and Y. Yin, *JHEP* **01**, 172 (2019), [arXiv:1808.03250 \[hep-ph\]](#).
- [45] A. Kumar, A. Majumder, and C. Shen, *Phys. Rev. C* **101**, 034908 (2020), [arXiv:1909.03178 \[nucl-th\]](#).
- [46] Z. Yang, Y. He, I. Moulton, and X.-N. Wang, *Phys. Rev. Lett.* **132**, 011901 (2024), [arXiv:2310.01500 \[hep-ph\]](#).
- [47] C. Park, S. Jeon, and C. Gale, *Nucl. Phys. A* **982**, 643 (2019), [arXiv:1807.06550 \[nucl-th\]](#).
- [48] Y. Tachibana *et al.* (JETSCAPE), *PoS Hard-Probes2018*, 099 (2018), [arXiv:1812.06366 \[nucl-th\]](#).
- [49] J. G. Milhano and K. Zapp, *Eur. Phys. J. C* **82**, 1010 (2022), [arXiv:2207.14814 \[hep-ph\]](#).
- [50] A. Kumar *et al.* (JETSCAPE), *Phys. Rev. C* **107**, 034911 (2023), [arXiv:2204.01163 \[hep-ph\]](#).
- [51] Y. Tachibana *et al.* (JETSCAPE), (2023), [arXiv:2301.02485 \[hep-ph\]](#).
- [52] T. Luo, Y. He, S. Cao, and X.-N. Wang, *Phys. Rev. C* **109**, 034919 (2024), [arXiv:2306.13742 \[nucl-th\]](#).
- [53] Soft emission patterns are recovered if in Eq. (3) the quark current is replaced by the real emission of a gluon with momentum $q = p' - p$:
- $$ig_s a_{ij} B_\mu \rightarrow \epsilon_\mu^*(q).$$
- [54] A. E. Chudakov, *Izv. Akad. Nauk SSSR, Ser. Fiz.*, 19:650 (1955).
- [55] L. Apolinário, J. G. Milhano, G. P. Salam, and C. A. Salgado, *Phys. Rev. Lett.* **120**, 232301 (2018), [arXiv:1711.03105 \[hep-ph\]](#).
- [56] J. a. Barata, A. V. Sadofyev, and C. A. Salgado, *Phys. Rev. D* **105**, 114010 (2022), [arXiv:2202.08847 \[hep-ph\]](#).
- [57] J. a. Barata, A. V. Sadofyev, and X.-N. Wang, *Phys. Rev. D* **107**, L051503 (2023), [arXiv:2210.06519 \[hep-ph\]](#).
- [58] J. a. Barata, X. Mayo López, A. V. Sadofyev, and C. A. Salgado, *Phys. Rev. D* **108**, 034018 (2023), [arXiv:2304.03712 \[hep-ph\]](#).
- [59] J. a. Barata, J. G. Milhano, and A. V. Sadofyev, *Eur. Phys. J. C* **84**, 174 (2024), [arXiv:2308.01294 \[hep-ph\]](#).
- [60] M. V. Kuzmin, X. Mayo López, J. Reiten, and A. V. Sadofyev, *Phys. Rev. D* **109**, 014036 (2024), [arXiv:2309.00683 \[hep-ph\]](#).
- [61] A. V. Sadofyev, M. D. Sievert, and I. Vitev, *Phys. Rev. D* **104**, 094044 (2021), [arXiv:2104.09513 \[hep-ph\]](#).
- [62] C. Andres, F. Dominguez, A. V. Sadofyev, and C. A. Salgado, *Phys. Rev. D* **106**, 074023 (2022), [arXiv:2207.07141 \[hep-ph\]](#).
- [63] Y. Mehtar-Tani and K. Tywoniuk, *JHEP* **01**, 031 (2013), [arXiv:1105.1346 \[hep-ph\]](#).
- [64] Y. He, T. Luo, X.-N. Wang, and Y. Zhu, *Phys. Rev. C* **91**, 054908 (2015), [Erratum: *Phys. Rev. C* **97**, 019902 (2018)], [arXiv:1503.03313 \[nucl-th\]](#).
- [65] K. C. Zapp, *Eur. Phys. J. C* **74**, 2762 (2014), [arXiv:1311.0048 \[hep-ph\]](#).
- [66] W. Ke and X.-N. Wang, *JHEP* **05**, 041 (2021), [arXiv:2010.13680 \[hep-ph\]](#).
- [67] S. Cao *et al.* (JETSCAPE), *Phys. Rev. C* **104**, 024905 (2021), [arXiv:2102.11337 \[nucl-th\]](#).
- [68] Z. Hulcher, D. Pablos, and K. Rajagopal, *Acta Phys. Polon. Supp.* **16**, 1 (2023), [arXiv:2208.13593 \[hep-ph\]](#).